

Calculated spin-orbit splitting of all diamond-like and zinc-blende semiconductors: Effects of $p_{1/2}$ local orbitals and chemical trends

Pierre Carrier¹ and Su-Huai Wei¹

¹*National Renewable Energy Laboratory, Golden CO 80401, USA*

(Dated: November 1, 2018)

We have calculated the spin-orbit (SO) splitting $\Delta_{SO} = \epsilon(\Gamma_{8v}) - \epsilon(\Gamma_{7v})$ for all diamond-like group IV and zinc-blende group III-V, II-VI, and I-VII semiconductors using the full potential linearized augmented plane wave method within the local density approximation. The SO coupling is included using the second variation procedure, including the $p_{1/2}$ local orbitals. The calculated SO splittings are in very good agreement with available experimental data. The corrections due to the inclusion of the $p_{1/2}$ local orbital are negligible for lighter atoms, but can be as large as ~ 250 meV for $6p$ anions. We find that (i) the SO splittings increase monotonically when anion atomic number increases; (ii) the SO splittings increase with the cation atomic number when the compound is more covalent such as in most III-V compounds; (iii) the SO splittings decrease with the cation atomic number when the compound is more ionic, such as in II-VI and the III-nitride compounds; (iv) the common-anion rule, which states that the variation of Δ_{SO} is small for common-anion systems, is usually obeyed, especially for ionic systems, but can break down if the compounds contain second-row elements such as BSb; (v) for IB-VII compounds, the Δ_{SO} is small and in many cases negative and it does not follow the rules discussed above. These trends are explained in terms of atomic SO splitting, volume deformation-induced charge renormalization, and cation-anion p - d couplings.

PACS numbers: 71.55.-i, 61.72.Vv; 78.20.Bh, 78.40.-q

I. INTRODUCTION

Spin-orbit (SO) splitting $\Delta_{SO} = \epsilon(\Gamma_{8v}) - \epsilon(\Gamma_{7v})$ at the top of the valence band of a semiconductor is an important parameter for the determination of optical transitions in these systems.^{1,2,3} It is also an important parameter to gauge the chemical environment and bonding of a semiconductor.^{1,4,5,6,7} Extensive studies of SO splitting, both theoretically^{8,9,10,11,12,13,14,15} and experimentally,^{16,17,18,19,20,21,22,23,24,25,26,27,28,29,30} have been carried out in the past. However, most of these studies focussed on a specific compound or a small group of similar compounds. Therefore, the general trends of the spin-orbit splitting in zinc-blende semiconductors is not very well established. From the experimental point of view, some of the data were measured more than 30 years ago,¹⁷ and the accuracy of these data is still under debate. For example, previous experimental data suggest that CdTe and HgTe have SO splittings Δ_{SO} at about 0.8 and 1.08 eV, respectively.¹⁷ These values have been used widely by experimental groups¹⁸ to interpret optical and magneto-optical transition data of CdTe, HgTe, and related alloys and heterostructures. However, recent experimental data suggest that Δ_{SO} for CdTe and HgTe are instead around 0.95 eV²⁷ and 0.91 eV.²⁶ Without basic understanding of the general trends of variation of Δ_{SO} in tetrahedral semiconductors, it is difficult to judge what should be the correct value of Δ_{SO} for CdTe and HgTe. There are also several non-conventional II-VI and III-V semiconductors that do not have a zinc-blende ground state (e.g., CdO, MgO, GaBi, InBi), but that do form zinc-blende alloys with other compounds, and are currently under intensive research as novel optoelectronic materials.^{31,32,33,34} Therefore, it is important

to know the spin-orbit splittings of these compounds in the zinc-blende phase and understand how they vary as a function of alloy concentration x in the alloy.

From the theoretical point of view, various approximations have been used to calculate and/or predict SO splitting Δ_{SO} . However, it is not clear how these approximations affect the calculated Δ_{SO} . For example, one of the most widely used procedures for calculating the SO coupling using the density functional theory³⁵ (DFT) and local density approximation^{36,37} (LDA) is the second-variation method^{38,39} used in many all-electron linearized augmented plane wave (LAPW) codes.^{40,41,42} In this approach, following the suggestion of Koelling and Harmon,³⁸ the Hamiltonian of the relativistic Dirac equation is separated into a “J-weighted-averaged” scalar relativistic Hamiltonian H_{SR} , in which the dependency on the quantum number κ [where $\kappa = \pm(j + 1/2)$, with $|j\rangle = |\vec{l} + \vec{s}\rangle = l \mp 1/2$] is removed from the full Hamiltonian, and a spin-orbit Hamiltonian H_{SO} with

$$H_{SO} = \frac{\hbar}{(2Mc)^2} \frac{1}{r} \frac{dV}{dr} (\vec{l} \cdot \vec{s}),$$

where

$$M = m + \frac{\epsilon - V}{2c^2}$$

is the relativistically enhanced electron mass, c is the speed of light, V is the effective potential, ϵ is the eigenvalue, and \vec{s} and \vec{l} are the Pauli spin and angular momentum operators, respectively. The scalar relativistic Hamiltonian, which includes the mass velocity and Darwin corrections, is solved first using standard diagonalization method for each spin orientation (or solved

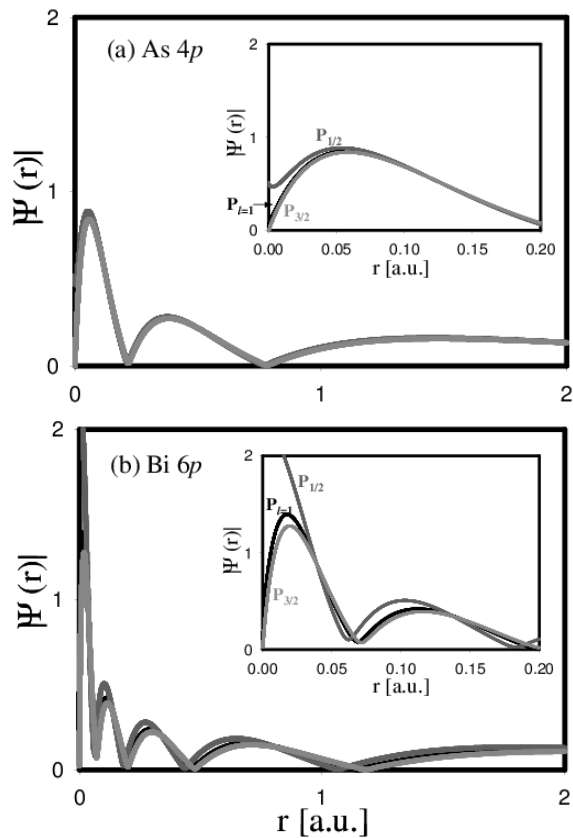


FIG. 1: Comparison of $p_{1/2}$, $p_{3/2}$, and $p_{l=1}$ orbitals in atomic As and Bi showing the large discrepancy between $p_{1/2}$ and the $p_{l=1}$ orbitals, especially for the heavier Bi atom.

just once if the system is not spin polarized). The SO Hamiltonian is included subsequently, in where the full Hamiltonian is solved using the scalar relativistic wavefunctions as basis set. Normally, only a small number of scalar relativistic wavefunctions are included in the second step, and only the spherical part of the potential within a muffin-tin sphere centered on each atomic site is used in the SO Hamiltonian. The advantage of the second-variation method is the physical transparency (e.g., it keeps spin as a good quantum number as long as possible) and the efficiency, because, in most cases in the second step, only a small number of basis functions are needed to have good agreement with solutions of fully relativistic Dirac equations. This approach has been shown to obtain Δ_{SO} that is in excellent agreement with experiments. For example, the calculated Δ_{SO} for GaAs is 0.34 eV compared with experimental data of 0.34 eV.¹⁷ However, one major approximation in the “J-weighted-averaged” treatment is the replacement of the two $p_{1/2}$ and $p_{3/2}$ orbitals by one $p_{l=1}$ orbital. Although this is a good approximation for atoms with low atomic number, it has been shown that such approximation fails for heavy atoms.^{39,43,44} The main reason for this failure is because the $p_{1/2}$ orbital has finite magnitude at the nuclear site, whereas the $l = 1$ orbital has zero magnitude at the nu-

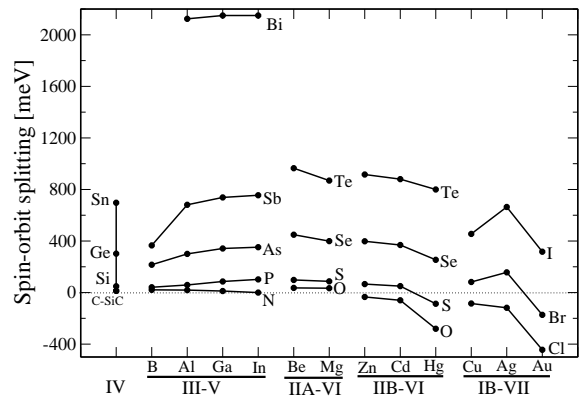


FIG. 2: Chemical trend of the spin-orbit splittings for all diamond-like group IV and zinc-blende group III-V, II-VI, and I-VII semiconductors, including the $p_{1/2}$ local orbitals. The graph corresponds to the data in column “LAPW+ $p_{1/2}$ ” of Tables I, II, and III.

clear site. Figure 1 plots the $p_{1/2}$, $p_{3/2}$, and $p_{l=1}$ orbitals for As ($Z=33$) and Bi ($Z=83$). As we can see, the $p_{1/2}$ orbital deviates significantly from the $p_{l=1}$ orbital near the origin. The error clearly increases as the atomic number increases, and is very large for heavier elements such as Bi. Therefore, the $p_{1/2}$ orbital is not very well represented near the nuclear site using the $p_{l=1}$ orbital, even with the addition of its energy derivative in the linearization procedure.⁴² Consequently, the SO splitting cannot be accurately evaluated, in general, with solely the $p_{l=1}$ orbital. However, no systematic studies have been done to evaluate the effect of the $p_{1/2}$ orbital on the calculated SO splitting Δ_{SO} .

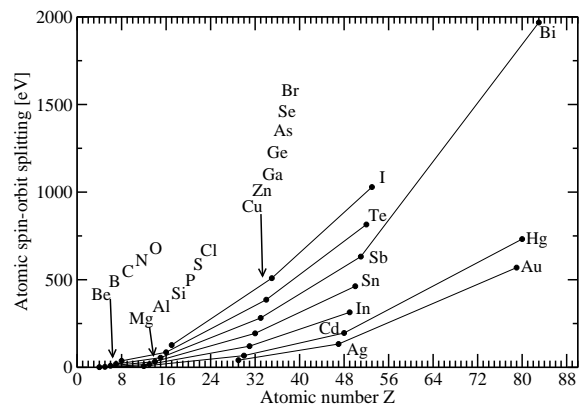


FIG. 3: Atomic spin-orbit splittings $\epsilon(p_{3/2}) - \epsilon(p_{1/2})$ for atoms studied in this paper. The spin-orbit splittings increase as a function of the atomic number Z . See Table IV for data subdivided according to their respective groups.

The objective of this paper is to do a systematic study of the SO splitting Δ_{SO} of all diamond-group IV and zinc-blende groups III-V, II-VI, and I-VII semiconductors using the first-principles band-structure method within the density functional formalism. We find that the cal-

culated SO splittings including the $p_{1/2}$ local orbital are in good agreement with available experimental data. The general chemical trends of the Δ_{SO} are revealed and explained in terms of atomic SO splittings, volume effects, and p - d coupling effects.

II. METHOD OF CALCULATIONS

The calculations are performed using the full potential linearized augmented plane wave (FLAPW) method as implemented in the WIEN2k code.^{40,42} The frozen core projector augmented wave (PAW) approach implemented in the VASP code^{45,46} is used for comparison. We used the Monkhost-Pack⁴⁷ $4 \times 4 \times 4$ \mathbf{k} points for the Brillouin zone integration. For the FLAPW method, SO coupling is included using the second-variation method performed with or without the $p_{1/2}$ local orbitals. Highly converged cutoff parameters in terms of the numbers of spherical harmonics inside the muffin-tin region and the plane waves in the interstitial region, as well as local orbitals for low-lying valence band states (anion s and cation d states), are used to ensure the full convergence of the calculated values. For the PAW method, high precision energy cutoffs have been chosen for all semiconductors (as large as 37 Rydberg for the nitrides and oxides).

In most cases, the band structure calculations are performed at the experimental lattice constants. For compounds that have only experimental lattice constant in the wurtzite structure, such as ZnO, we assume that zinc-blende ZnO has the same volume as in its wurtzite structure.¹⁶ For BSb, the (Al, Ga, In)Bi, and the (Be, Mg, Cd, Hg)O, that does not have either zinc-blende or wurtzite experimental structure parameters, the LDA-calculated lattice constants are used. For the silver halides and the gold halides, the LDA lattice constants have been corrected according to the small discrepancy between LDA and experiment values of AgI (more precisely, 0.088 Å have been added to the LDA lattice constants of silver halides and gold halides). The LDA-calculated lattice constants are expected to be reliable. For example, our predicted³² lattice constant of GaBi is $a = 6.324$ Å, whereas recent experimental observation³⁴ finds a value around 6.33 ± 0.06 Å, in good agreement with our prediction. All the lattice constants used in our calculation are listed in Tables I, II, and III.

III. EFFECT OF THE $p_{1/2}$ LOCAL ORBITAL

Tables I, II, and III present the calculated SO splittings data for all diamond-like group IV and zinc-blende groups III-V, II-VI, and I-VII semiconductors. The calculated values are obtained with or without the $p_{1/2}$ local orbitals. We find that including the $p_{1/2}$ local orbital provides a better variation basis for the Γ_{7v} state, lowers the eigen energy, and, therefore, increases the SO splitting

TABLE I: Calculated spin-orbit splitting Δ_{SO} for all diamond group IV and zinc-blende group III-V semiconductors, using the FLAPW method with or without the $p_{1/2}$ local orbitals and the frozen-core PAW method. Our results are compared with available experimental data. Our error analysis suggests that the uncertainty of the LDA calculated value is less than 20 meV.

Comp.	a (Å)	Δ_{SO} [meV]			
		LAPW	LAPW+ $p_{1/2}$	PAW	exper.
IV					
C	3.5668	13	13	14	13 ^a
SiC	4.3596	14	14	15	10 ^b
Si	5.4307	49	49	50	44 ^c
Ge	5.6579	298	302	302	296 ^b
α -Sn	6.4890	669	697	689	800 ^c
III-V					
BN	3.6157	21	21	22	—
BP	4.5383	41	41	42	—
BA _s	4.7770	213	216	212	—
BSb	5.1982	348	366	346	—
AlN	4.3600	19	19	19	19 ^d
AlP	5.4635	59	59	62	—
AlAs	5.6600	296	300	305	275 ^b , 300 ^c
AlSb	6.1355	658	681	679	750 ^b , 673 ^c
AlBi	6.3417	1 895	2 124	2 020	—
GaN	4.5000	12	12	12	11 ^c , 17 ^d
GaP	5.4505	86	86	88	80 ^c
GaAs	5.6526	338	342	342	341 ^c
GaSb	6.0951	714	738	722	752 ^c , 730 ^e
GaBi	6.3240	1 928	2 150	2 070	—
InN	4.9800	-1	0	0	5 ^d
InP	5.8687	100	102	104	108 ^c , 99 ^f
InAs	6.0583	344	352	355	371 ^b , 380 ^c
InSb	6.4794	731	755	754	803 ^b , 850 ^c , 750 ^g
InBi	6.6860	1 917	2 150	2 089	—

^a Reference 50.

^b Reference 17.

^c Reference 16.

^d Reference 30.

^e Reference 19.

^f Reference 20.

^g Reference 21.

$\Delta_{SO} = \epsilon(\Gamma_{8v}) - \epsilon(\Gamma_{7v})$. The correction due to the $p_{1/2}$ orbital increases as the atomic number increases. Since the VBM consists of mostly anion p state, the dependence is more on anion atomic numbers. We find that corrections due to the inclusion of the $p_{1/2}$ local orbital (for both anions and cations) are negligible for lighter atoms, are ~ 10 meV for $4p$ anions, ~ 40 meV for $5p$ anions and can be as large as ~ 250 meV for $6p$ anions. Thus, for Bi compounds (AlBi, GaBi, and InBi), large errors could be introduced if the $p_{1/2}$ local orbital is not included.³² In all the cases, inclusion of $p_{1/2}$ local orbital brings a better agreement between the calculated Δ_{SO} and available

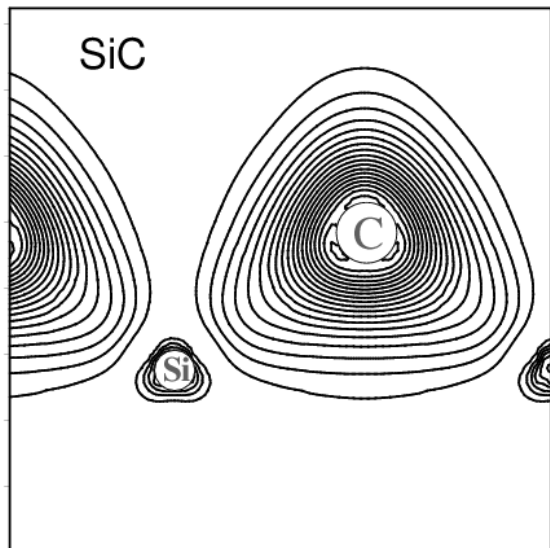


FIG. 4: Charge distribution at the VBM for SiC. The charges are mostly distributed on the carbon atom site.

experimental data.

IV. CHEMICAL TRENDS

Figure 2 shows the general chemical trends of the calculated SO splittings Δ_{SO} for all diamond-like group IV and zinc-blende III-V, II-VI, and I-VII semiconductors, with inclusion of the $p_{1/2}$ local orbitals. We find that (i) the SO splittings increase monotonically when anion atomic number increases; (ii) the SO splittings increase with the cation atomic number when the compound is more covalent, such as in most III-V compounds; (iii) the SO splittings decrease with the cation atomic number when the compound is more ionic, such as in II-VI and the III-nitride compounds; (iv) for compounds with the same principal quantum number, Δ_{SO} increases as the ionicity of the compounds increases. Finally, (v) the halides (IB-VII) constitute a special case because the VBM in IB-VII is no longer an anion p dominant state.⁴⁸ Therefore, IB-VII compounds do not follow the rules discussed above.

To understand these chemical trends, we will first discuss the factors that can affect the SO splitting Δ_{SO} for the systems studied here. **(a) Dependence on the atomic number.** The atomic SO splitting between the $p_{3/2}$ and $p_{1/2}$ states increases as a function of atomic number Z . Table IV gives the calculated splitting of the atomic fine structures, $\epsilon(p_{3/2}) - \epsilon(p_{1/2})$, as a function of the atomic number Z in their respective groups. Figure 3 (related to Table IV) shows the variation of the atomic spin-orbit splittings as a function of the atomic numbers, for all atoms considered. The spin-orbit splittings increase with the atomic number, as expected.⁴⁹ The increases follow approximately a power law with

TABLE II: Calculated spin-orbit splitting Δ_{SO} for all IIA-VI and IIB-VI semiconductors, using the FLAPW method, with or without the $p_{1/2}$ local orbitals, and the frozen-core PAW method. The lattice constants with a \star corresponds to one at their LDA energy minimum (for ZnO^{**}, the lattice constant of the zinc-blende structure is chosen so that its volume is equal to that in the wurtzite structure). Our results are compared with available experimental data. Our error analysis suggests that due to the overestimation of the p - d hybridization, our calculated Δ_{SO} is underestimated by 30, 40, and 110 meV for Zn, Cd, and Hg compounds, respectively. For other compounds, the LDA error is estimated to be less than 20 meV.

Comp.	a (Å)	Δ_{SO} [meV]			exper.
		LAPW	LAPW+ $p_{1/2}$	PAW	
<u>IIA-VI</u>					
BeO	3.7654 [*]	36	36	38	—
BeS	4.8650	98	98	98	—
BeSe	5.1390	445	449	447	—
BeTe	5.6250	927	965	944	—
MgO	4.5236 [*]	34	34	34	—
MgS	5.6220	87	87	87	—
MgSe	5.8900	396	399	396	—
MgTe	6.4140	832	869	854	945 ^a
<u>IIB-VI</u>					
ZnO	4.5720 ^{**}	-34	-34	-37	-4 ^b
ZnS	5.4102	66	66	64	65 ^c , 86 ^d
ZnSe	5.6676	393	398	392	420 ^{c,e} , 400 ^d
ZnTe	6.0890	889	916	898	910 ^d , 950 ^a
CdO	5.0162 [*]	-59	-60	-58	—
CdS	5.8180	50	50	46	62 ^d , 56 ^b
CdSe	6.0520	364	369	370	416 ^d , 390 ^e
CdTe	6.4820	848	880	865	810 ^c , 800 ^d , 900 ^f
HgO	5.1566 [*]	-285	-281	-292	—
HgS	5.8500	-100	-87	-108	—
HgSe	6.0850	235	254	238	450 ^c , 396 ^d , 300 ^g
HgTe	6.4603	762	800	781	1080 ^c , 910 ^g

^a Reference 22.

^b Reference 23.

^c Reference 17.

^d Reference 16.

^e Reference 24.

^f Reference 25.

^g Reference 26.

$\Delta_{SO}(p_{3/2} - p_{1/2}) \propto Z^\alpha$, where α is close to 2. **(b) Dependence on the volume.** As the volume of the compound decreases, the charge distribution in the crystal is renormalized. The bonds become more covalent. More charge is pushed into a region near the nuclei. Because the SO coupling is larger near the nuclear site, the SO splitting Δ_{SO} usually increases as the volume decreases. **(c) Dependence on the cation valence d orbital.** The VBM in a majority of zinc-blende semiconductors consists of mostly anion p and a smaller amount of cation p orbitals. By symmetry, the VBM state in zinc-blende

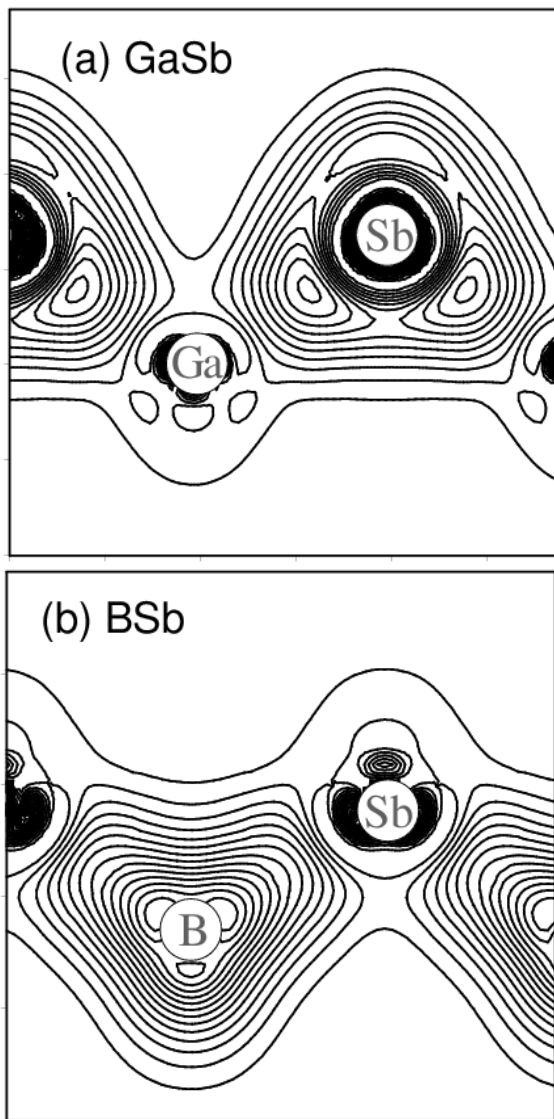


FIG. 5: Charge density of the VBM state for GaSb and BSb, showing that for BSb the role of cation and anion is reversed.

structure can couple with the cation t_{2d} orbitals. The cation t_{2d} orbital has a negative contribution^{1,15} to the SO splitting Δ_{SO} (i.e., the Γ_{8v} is below the Γ_{7v} state). Thus, large mixing of heavy cation d orbitals in VBM can reduce Δ_{SO} .

Using the discussion above, we can now understand the general chemical trends of the SO splitting Δ_{SO} .

(i) The SO splittings increase monotonically when anion atomic number increases. For example, Δ_{SO} increases from 13 \rightarrow 49 \rightarrow 302 \rightarrow 697 meV when the atomic number increases from C \rightarrow Si \rightarrow Ge \rightarrow α -Sn; from 12 \rightarrow 86 \rightarrow 342 \rightarrow 738 \rightarrow 2150 meV when the anion atomic number increases from GaN \rightarrow GaP \rightarrow GaAs \rightarrow GaSb \rightarrow GaBi; from -60 \rightarrow 50 \rightarrow 369 \rightarrow 880 meV when the anion atomic number increases from CdO \rightarrow CdS \rightarrow CdSe \rightarrow CdTe; from -85 \rightarrow 82 \rightarrow 455 when the anion atomic number increases from CuCl \rightarrow CuBr \rightarrow CuI. This is

TABLE III: Calculated spin-orbit splitting Δ_{SO} for all IB-VII compounds, using the FLAPW method, with or without the $p_{1/2}$ local orbitals, and the frozen-core PAW method. Our results are compared with available experimental data. We use experimental lattice constants^{48,52,53} for CuX (X= Cl, Br, I) and AgI. The lattice constants for the other AgX and AuX compounds are estimated from calculated LDA lattice constants and experimental lattice constant of AgI. Due to the overestimation of the d character in the VBM, the LDA underestimate the Δ_{SO} by 20, 60, and 170 meV for chlorides, bromides, and iodides, respectively.

Compound	a (Å)	Δ_{SO} [meV]			
		LAPW	LAPW+ $p_{1/2}$	PAW	exper.
IB-VII					
CuCl	5.4057	-85	-85	-85	-69 ^a
CuBr	5.6905	80	82	86	147 ^a
CuI	6.0427	440	455	466	633 ^a
AgCl	5.8893*	-119	-118	-122	—
AgBr	6.1520*	155	157	158	—
AgI	6.4730	643	664	658	837 ^a
AuCl	5.7921*	-444	-444	-446	—
AuBr	6.0517*	-177	-173	-178	—
AuI	6.3427*	294	317	317	—

^a References 54 and 55.

because the VBM has large anion p character, and the atomic SO splitting of the anion valence p state increases with the atomic number (see Table IV). One of the interesting case is SiC. The calculated Δ_{SO} of 14 meV for SiC is very close to the one of diamond (13 meV), indicating that SiC is a very ionic material with its VBM containing mostly C character. Figure 4 depicts the contour plot of the charge distribution at the VBM for SiC, which shows that the VBM charge is located on the carbon atom site.

(ii) The SO splittings increase with the cation atomic number when the compound is more covalent, such as in most III-V compounds. For example, Δ_{SO} increases from 216 \rightarrow 300 \rightarrow 342 \rightarrow 352 meV when the atomic number increases from BAs \rightarrow AlAs \rightarrow GaAs \rightarrow InAs; from 366 \rightarrow 681 \rightarrow 738 \rightarrow 755 meV when the atomic number increases from BSb \rightarrow AlSb \rightarrow GaSb \rightarrow InSb. This is because for covalent III-V compounds, the VBM contains significant amount of cation p orbitals. Therefore, when the cation atomic number increases, the SO splitting Δ_{SO} also increases. It is interesting to note that Δ_{SO} for BX (X=P, As, and Sb) is significantly smaller than that for their corresponding common-anion compounds. For example, $\Delta_{SO}(\text{BSb})=366$ meV is only about half of the value of $\Delta_{SO}(\text{GaSb})=738$ meV. This is because boron is much more electronegative than other group III elements. Thus, BX compounds are much more covalent than the other III-V semiconductors. Figure 5 compares the charge distribution of the VBM states for BSb and GaSb. We see that for GaSb, most of the VBM charge is on Sb atom site, whereas for BSb, a large portion of the

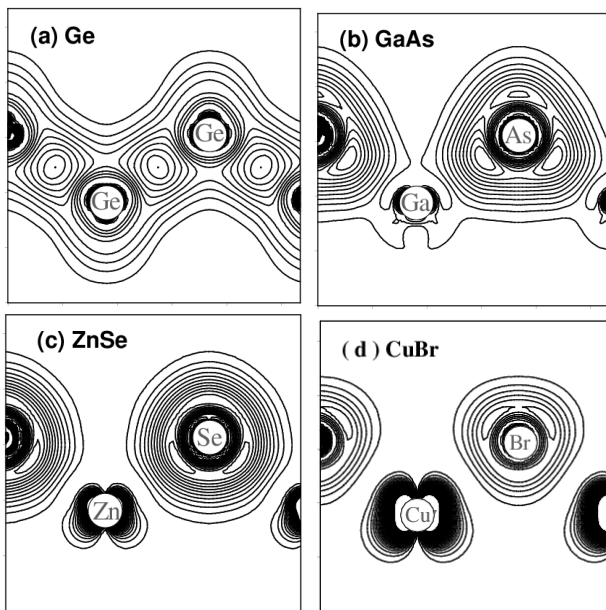


FIG. 6: Charge density of the VBM states for Ge, GaAs, ZnSe, and CuBr showing that as ionicity increases, the charge is more localized on the anion site. For ZnSe and CuBr, it also shows antibonding d character on the Zn and Cu sites, respectively.¹⁵

VBM charge is on the B atom site. Because boron has a small atomic number ($Z=5$), the SO splitting of B $2p$ states is very small, leading to very small Δ_{SO} for BX. This indicates that the common-anion rule, which states that the variation of Δ_{SO} is small for common anion systems, does not apply to all BX, which are extremely covalent.

(iii) The SO splittings decrease with the cation atomic number when the compound is more ionic, such as in II-VI and III-nitride compounds. For example, Δ_{SO} decreases from 449 \rightarrow 399 meV when the atomic number increases from BeSe \rightarrow MgSe; from 965 \rightarrow 869 meV when the atomic number increases from BeTe \rightarrow MgTe; from 398 \rightarrow 369 \rightarrow 254 meV when the atomic number increases from ZnSe \rightarrow CdSe \rightarrow HgSe; from 21 \rightarrow 19 \rightarrow 12 \rightarrow 0 meV when the atomic number increases from BN to AlN \rightarrow GaN \rightarrow InN. This is because for ionic II-VI and III-nitride systems, the VBM is mostly an anion p state, thus the Δ_{SO} is not sensitive to the cation atomic number or potential. However, when cation atomic number decreases, say from Mg to Be, the volume of the compounds decreases (Table II), and therefore, due to the charge renormalization effect, the Δ_{SO} increases. In particular, for the IIB-VI systems and the III-nitrides, the coupling between cation d and anion p also plays an important role in the observed trend, because the p - d hybridization is significant in these systems (See Fig. 6c). The p - d hybridization reduces Δ_{SO} ,^{1,15} and the effect increases when cation atomic number increases. This explains why $\Delta_{SO}(\text{HgX})$ (for X=O, S, Se, Te) is smaller than $\Delta_{SO}(\text{CdX})$, even though they have similar volume,

TABLE IV: Atomic SO splitting $\epsilon(p_{3/2}) - \epsilon(p_{1/2})$ for the compounds of Tables I, II, and III, according to their atomic groups. The data are also depicted in Fig. 3, as a function of atomic numbers Z .

element	atomic number	$\epsilon(p_{3/2}) - \epsilon(p_{1/2})$ [meV]
IIB		
Cu	Z=29	41
Ag	Z=47	133
Au	Z=79	569
IIA		
Be	Z=4	1
Mg	Z=12	7
IIB		
Zn	Z=30	67
Cd	Z=48	196
Hg	Z=80	732
III		
B	Z= 5	3
Al	Z=13	17
Ga	Z=31	121
In	Z=49	314
IV		
C	Z= 6	9
Si	Z=14	33
Ge	Z=32	194
Sn	Z=50	463
V		
N	Z= 7	19
P	Z=15	55
As	Z=33	282
Sb	Z=51	632
Bi	Z=83	1 968
VI		
O	Z= 8	37
S	Z=16	86
Se	Z=34	386
Te	Z=52	815
VII		
Cl	Z=17	127
Br	Z=35	509
I	Z=53	1 029

and why $\Delta_{SO}(\text{InN})$ is smaller than $\Delta_{SO}(\text{GaN})$. Note that negative Δ_{SO} can exist in some of the compounds such as ZnO, CdO, and HgO where the anion is light, so their p orbitals have only a small contribution to Δ_{SO} , but the negative contribution of the cation d orbital is large.

(iv) For compounds with the same principal quantum number n , Δ_{SO} increases as the ionicity of the compound increases. For example, for $n = 2$, from C \rightarrow BN \rightarrow BeO, the SO splittings Δ_{SO} increase from 13 \rightarrow 21 \rightarrow 36 meV; for $n = 3$, from Si \rightarrow AlP \rightarrow MgS, the SO splittings increase from 49 \rightarrow 59 \rightarrow 87 meV; for $n = 4$, from Ge \rightarrow GaAs \rightarrow ZnSe, the SO splittings increase from 302 \rightarrow 342 \rightarrow to 398 meV; for $n = 5$, from α -Sn \rightarrow InSb \rightarrow CdTe, the SO splittings increase from 697 \rightarrow 755 \rightarrow 880 meV. The reason for this increase can be understood from plots in Fig. 6, which show the charge distribution of the VBM states of Ge, GaAs, and ZnSe.

As the system changes from group IV \rightarrow III-V \rightarrow II-VI, the compound becomes more ionic and the VBM becomes more localized on the anion site with increasing atomic number, thus Δ_{SO} increases. It is interesting to note that the differences of Δ_{SO} between the II-VI, the III-V, and the group IV compounds in the same row increases as n increases (almost doubles when n increases by one). This is explained by the fact that the atomic number Z almost doubles when n is increased by one, whereas the atomic SO splitting is proportional to Z^α with α close to 2 (See Table IV and the discussion above); thus, the difference is proportional to Z .

(v) The $A^{IB}X^{VII}$ halides ($A^{IB} = \text{Cu, Ag, Au}$; $X^{VII} = \text{Cl, Br, I}$) constitute a group of special compounds that do not follow the rules discussed above. For example, when moving from ZnSe to CuBr with increased ionicity (see Figure 6), the SO splitting of CuBr (82 meV) is much smaller than that for ZnSe (398 meV). The SO splitting of AgI (664 meV) is also much smaller than that of CdTe (880 meV). Furthermore, many of the IB-VII compounds (CuCl, AgCl, AuCl, and CuBr) have negative SO splittings, and for these ionic compounds CuX^{VII} has much smaller SO splittings than AgX^{VII} and AuX^{VII} . The origin of these anomalies is due to the fact that for most of the IB-VII compounds the VBM is no longer an anion p dominated state. Instead, they are cation d states strongly hybridized with the anion p state. For instance, in Figure 6(d) we show that the VBM of CuBr has a very pronounced antibonding d character at the cation Cu site. Because the d state has negative Δ_{SO} , this explains why some of the IB-VII compounds have negative Δ_{SO} . Furthermore, because Cu $3d$ level is much higher than Ag $4d$ and Au $5d$ levels, the VBM of Cu halides contains more cation d character than Ag and Au compounds. This explains why Cu halides have much smaller Δ_{SO} than the Ag and Au common anion halides.

V. COMPARISON WITH EXPERIMENTS

Our calculated results with the $p_{1/2}$ local orbitals are compared with experimental data.^{16,17,18,19,20,21,22,23,24,25,26,27,28,29,30} For most semiconductors the agreement is very good. For example, the calculated value for diamond (13 meV) is in very good agreement with the recent experimentally derived value of 13 meV.⁵⁰ The experimental value for SiC in the zinc-blende structure (10 meV)^{14,17} is smaller than the one for C, therefore, does not follow the chemical trend. We suggest that the measured value is possibly underestimated. For most semiconductors, the difference between theory and experiment is usually less than 20 meV. However, there are several noticeable cases in which the difference is much larger. For example, for α -Sn, the calculated value is 697 meV, whereas the value in experiment data¹⁶ is \sim 800 meV. For HgTe the calculated value at 800 meV is much smaller than the widely used experimental value¹⁷ of 1080 meV. To

understand the origin of the discrepancy, we performed the following tests. First, we considered a different numerical approach, i.e., the frozen core PAW method as implemented in the VASP code to calculate the SO splitting Δ_{SO} . Despite the large difference in the way the SO coupling is implemented in the calculations, we find that the Δ_{SO} calculated with the PAW method are very similar to that obtained with the FLAPW method. For α -Sn and HgTe, the results obtained by the PAW method are 689 and 781 meV, respectively, in good agreement with the FLAPW-calculated values of 697 and 800 meV. Next, we estimated the effect of p - d coupling. It has been argued that the LDA-calculated cation d orbitals are too shallow,¹⁵ so p - d hybridization at the VBM is overestimated, which may lead to smaller calculated Δ_{SO} . To verify if this is the possible reason, we performed the following calculations. (i) After obtaining the converged LDA potential, we removed the cation d orbital from the basis set to calculate the Δ_{SO} . We find that for α -Sn, this procedure has no effect on the calculated Δ_{SO} . This is consistent with the fact that for this compound, the cation d and anion p separation is large enough that the amount of cation d orbital at the VBM is not sufficient to affect the calculated Δ_{SO} . For ZnTe, CdTe, and HgTe, removing the cation d orbital increases the Δ_{SO} by 48, 63, and 253 meV, respectively. These values are the upper limit on the possible effect of p - d coupling on the calculated Δ_{SO} . (ii) To get more reliable estimates on the LDA error of the calculated Δ_{SO} , we added an external potential⁵¹ on the cation muffin-tin sphere to push down the cation d orbitals such that the calculated cation binding energy is close to the experimental photoemission data.¹⁵ In this case, the calculated Δ_{SO} is 0.94, 0.91, and 0.90 eV for ZnTe, CdTe, and HgTe, respectively. The above analysis demonstrates that the possible LDA error in calculating Δ_{SO} is less than 30, 40, and 110 meV for Zn, Cd, and Hg compounds, respectively, and much smaller for other compounds.

Our analysis above suggests that Δ_{SO} for α -Sn and HgTe should be around 0.70 and 0.90 eV, respectively, smaller than the experimental values of 0.80 and 1.08 eV, respectively. The origin of this discrepancy is still not very clear. But we notice that α -Sn and HgTe are semimetals, i.e., the Γ_{6c} state is below the VBM. This makes the accurate measurement of the Δ_{SO} for these compounds more challenging. Indeed, recent measurements²⁶ of Δ_{SO} for HgTe show that it has a value of 0.9 eV, in good agreement with our predicted value. We also notice that the recent reported experimental SO splitting for InSb,²¹ which has a very small band gap (0.24 eV), agrees well with our calculation. Further experimental studies are needed to clarify these issues.

VI. SUMMARY

In summary, we have studied systematically the SO splitting Δ_{SO} of all diamond-like group IV and zincblende group III-V, II-VI, and I-VII semiconductors using the first-principles band structure method. We studied the effect of the $p_{1/2}$ local orbitals on the calculated Δ_{SO} . The general trends of Δ_{SO} of the semiconductors are revealed and explained in terms of atomic SO splitting, volume deformation-induced charge renormalization, and cation-anion p - d couplings. In most cases,

our calculated results are in good agreement with the experimental data. The differences between our calculated value for α -Sn and HgTe, and to a lesser degree for InAs and GaSb, are highlighted. Experiments are called for to test our predictions.

VII. ACKNOWLEDGMENTS

This work was supported by the U.S. Department of Energy, Grant No. DE-AC36-99G010337.

-
- ¹ M. Cardona, in *Solid State Physics*, edited by F. Seitz, D. Turnbull, and E. Ehrenreich (Academic, New York, 1969), Vol. 11.
- ² S.-H. Wei and A. Zunger, *Appl. Phys. Lett.* **64**, 1676 (1994).
- ³ A. Janotti and S.-H. Wei, *Appl. Phys. Lett.* **81**, 3957 (2002).
- ⁴ J. C. Phillips, *Bonds and Bands in Semiconductors* (Academic, New York, 1973).
- ⁵ S.-H. Wei and A. Zunger, *Phys. Rev. B* **39**, 6279 (1989).
- ⁶ J. A. Van Vechten, O. Berolo, and J. C. Woolley, *Phys. Rev. Lett.* **29**, 1400 (1972).
- ⁷ P. Parayanthal and F. H. Pollak, *Phys. Rev. B* **28**, 3632 (1983).
- ⁸ M. Cardona and N. E. Christensen, *Solid State Commun.* **116**, 421 (2000).
- ⁹ G. G. Wepfer, T. C. Collins, and R. N. Euwema, *Phys. Rev. B* **4** 1296 (1971).
- ¹⁰ M. Cardona, *Modulation Spectroscopy* (Academic, New York, 1969).
- ¹¹ H. C. Poon, Z. C. Feng, Y. P. Feng, and M. F. Li, *J. Phys.: Cond. Matter* **7**, 2783 (1995).
- ¹² M. Willatzen, M. Cardona, and N. E. Christensen, *Phys. Rev. B* **51**, 17992 (1995).
- ¹³ Y. Al-Douri, R. Khenata, Z. Chelahi-Chikr, M. Driz, and H. Aourag, *J. Appl. Phys.* **94**, 4502 (2003).
- ¹⁴ C. Persson and U. Lindelfelt, *J. Appl. Phys.* **82**, 5496 (1997).
- ¹⁵ S.-H. Wei and A. Zunger, *Phys. Rev. B* **37**, 8958 (1988).
- ¹⁶ *Semiconductors: Basic Data*, second edition, edited by O. Madelung (Springer, Berlin, 1996).
- ¹⁷ *Landolt-Börnstein: Numerical Data and Functional Relationships in Science and Technology*, Vol. III/17a,b, edited by O. Madelung, M. Schulz, and H. Weiss (Springer, Berlin, 1982).
- ¹⁸ K. Ortner, X. C. Zhang, A. Pfeuffer-Jeschke, C. R. Becker, G. Landwehr, and L. W. Molenkamp, *Phys. Rev. B* **66**, 075322 (2002).
- ¹⁹ B. J. Parsons, H. Piller, Program and Abstract of the 3rd Materials Science Symposium, Electronic Density of States, 1969, Gaithersburg, MD, USA.
- ²⁰ K. Losch and J. U. Fischbach, *Phys. Stat. Sol. A* **33**, 473 (1976).
- ²¹ Ch. Jung and P. R. Bressler, *J. Elect. Spec. and Rel. Phenom.* **78**, 503 (1996).
- ²² B. Montegu, A. Laugier, and D. Barbier, *Phys. Rev. B* **19**, 1920 (1979); For MgTe, the SO splitting is the extrapolated value from $\text{Mg}_x\text{Zn}_{1-x}\text{Te}$ samples, where $x \leq 0.407$. The value for MgTe is overestimated by 50 meV, corresponding to their overestimation in ZnTe.
- ²³ Derived using the quasicubic model [J. J. Hopfield, *J. Phys. Chem. Solids* **15**, 97 (1960)] and the data in Ref. 16.
- ²⁴ Y. D. Kim, M. V. Klein, S. F. Ren, Y. C. Chang, H. Luo, N. Samarth, and J. K. Furdyna, *Phys. Rev. B* **49**, 7262 (1994).
- ²⁵ D. T. F. Marple and H. Ehrenreich, *Phys. Rev. Lett.* **8**, 87 (1962).
- ²⁶ C. Janowitz, N. Orłowski, R. Manzke, Z. Golacki, *J. Alloys and Compounds* **328**, 84 (2001).
- ²⁷ D. W. Niles and H. Höchst, *Phys. Rev. B* **43**, 1492 (1991).
- ²⁸ F. Herman, C. D. Kuglin, K. F. Cuff, and R. L. Kortum, *Phys. Rev. Lett.* **11**, 541 (1963).
- ²⁹ J. Wu, W. Walukiewicz, K. M. Yu, J. W. Ager III, E. E. Haller, I. Miotkowski, A. K. Ramdas, C.-H. Su, I. K. Sou, R. C. C. Perera, and J. D. Denlinger, *Phys. Rev. B* **67**, 035207 (2003).
- ³⁰ I. Vurgaftman and J. R. Meyer, *J. Appl. Phys.* **94**, 3675 (2003).
- ³¹ K. Oe and H. Okamoto, *Jpn. J. Appl. Phys.* **37**, Part 2, L1283 (1998).
- ³² A. Janotti, S.-H. Wei, and S. B. Zhang, *Phys. Rev. B* **65**, 115203 (2002). In this paper, SO coupling for GaBi and InBi is calculated without the $p_{1/2}$ orbitals.
- ³³ Th. Gruber, C. Kirchner, R. Kling, F. Reuss, A. Waag, F. Bertram, D. Forster, J. Christen, and M. Schreck, *Appl. Phys. Lett.* **83**, 3290 (2003).
- ³⁴ S. Tixier, M. Adamczyk, T. Tiedje, S. Francoeur, A. Mascarenhas, P. Wei, and F. Schiettekatte, *Appl. Phys. Lett.* **82**, 2245 (2003).
- ³⁵ P. Hohenberg and W. Kohn, *Phys. Rev.* **136**, B864 (1964).
- ³⁶ W. Kohn and L. J. Sham, *Phys. Rev.* **140**, A1133 (1965).
- ³⁷ J. P. Perdew and Wang Yue, *Phys. Rev. B* **33**, 8800 (1986).
- ³⁸ D. D. Koelling and B. N. Harmon, *J. Phys. C* **10**, 3107 (1977).
- ³⁹ A. H. MacDonald, W. E. Pickett, and D. D. Koelling, *J. Phys. C* **13**, 2675 (1980).
- ⁴⁰ P. Blaha, K. Schwarz, and J. Luitz, *WIEN2k*, Vienna University of Technology 1997. [Improved and updated Unix version of the original copyrighted WIEN code, which was published by P. Blaha, K. Schwarz, P. Sorantin, and S. B. Trickey, *Comput. Phys. Commun.* **59**, 399 (1990).].
- ⁴¹ S.-H. Wei and H. Krakauer, *Phys. Rev. Lett.* **55**, 1200 (1985), and reference therein.
- ⁴² D.J. Singh, *Planewaves, Pseudopotentials and the LAPW*

- Method*, (Kluwer Academic, Norwell, 1994).
- ⁴³ L. Nordström, J. M. Wills, P. H. Andersson, P. Söderlind, and O. Eriksson, Phys. Rev. B **63**, 035103 (2000).
- ⁴⁴ J. Kuneš, P. Novák, R. Schmid, P. Blaha, and K. Schwarz, Phys. Rev. B **64**, 153102 (2001).
- ⁴⁵ G. Kresse and J. Furthmüller, computer code VASP 4.6 (Vienna University of Technology, Vienna, 1997) [Improved and updated Unix version of the original copyrighted VASP/VAMP code, which was published by G. Kresse and J. Furthmüller, Comput. Mater. Sci. **6**, 15 (1996)]. We used Version 4.6.17.
- ⁴⁶ P. E. Blöchl, Phys. Rev. B **50**, 17953 (1994).
- ⁴⁷ H. J. Monkhorst and J. D. Pack, Phys. Rev. B **13**, 5188 (1976).
- ⁴⁸ A. Blacha, N. E. Christensen, and M. Cardona, Phys. Rev. B **33**, 2413 (1986).
- ⁴⁹ G. Baym, Lectures on Quantum Mechanics (Addison-Wesley, Reading, 1990).
- ⁵⁰ J. Serrano, M. Cardona, and T. Ruf, Solid State Commun, **113**, 411 (2000).
- ⁵¹ S.-H. Wei and P. Carrier, J. Cryst. Growth, to be published.
- ⁵² Y. Ma, J. S. Tse, and D. D. Klug, Phys. Rev. B **69**, 064102 (2004).
- ⁵³ S. Hull and D. A. Keen, Phys. Rev. B **50**, 5868 (1994).
- ⁵⁴ M. Cardona, Phys. Rev. **129**, 69 (1963).
- ⁵⁵ A. Blacha, M. Cardona, N. E. Christensen, S. Ves, and H. Overhof, Solid State Commun. **43**, 183 (1982).